Archaeological and Anthropological Sciences (2023) 15:138
https://doi.org/10.1007/s12520-023-01840-2

RESEARCH

Understanding the provenance and production process of historic mortars—a novel approach employing calcareous nannofossils

Janina Falkenberg[1] · Ulrich Kaplan[2] · Joerg Mutterlose[1]

Received: 25 June 2023 / Accepted: 8 August 2023 / Published online: 26 August 2023

Abstract

Limestones ($CaCO_3$) have been an important source for masonry and mortars throughout approx. 10,000 years of human history. They are often composed of calcitic shells of minute marine algae, known as calcareous nannofossils. The 0.25–30-µm large calcitic skeletons of these primary producers have been well documented from various archaeological materials including building stones of masonry. Surprisingly, these tiny microfossils were recently also observed in medieval mortars and mortar-based materials, even though the carbonate-based source rocks of the mortars have been heated in kilns for quicklime production. Burning experiments of carbonate-rich sedimentary rocks, containing well-preserved and abundant calcareous nannofossils, documented a deteriorating preservation and a decrease of diversity and relative abundance of the nannofossils with increasing temperatures.

Alongside the lime-based binder historic mortars often contain under- and overburnt lime lumps and carbonate-rich aggregates; the latter were added after the heating process. Lime lumps and aggregates offer additional, so far not yet fully understood information on the burning process. Here, calcareous nannofossils were studied in ultra-thin sections of historic mortars, resulting in the separate analysis of the binder, lime lumps and aggregates. The findings allow (i) a more precise provenance of the limestones and (ii) a more accurate reconstruction of the temperatures reached during historic quicklime production. Our study thus improves the provenance analysis approach of limestones and sheds light on historic technology of mortar production by using calcareous nannofossils.

Keywords Historic mortar · Provenance · Ancient technology · Calcination · Heating temperature · Calcareous nannofossils

Introduction

Mortars, which are globally used as a binding agent for the construction of buildings, are composed of a binder, aggregates and additives. The binder (lime, cement) fixes the solid particles and the aggregates (sand, rock fragments) fasten the hardening process and provide strength and durability. Additives like ceramic tiles and pozzolana (e.g. volcanic ash, natural materials consisting of silica and alumina) increase the material properties of the mortars like the hydraulicity (the hardening in wet conditions or underwater). The historically oldest binders used are lime, gypsum and mud. The oldest findings of lime as a binder go back to the Neolithic as documented from the Near East (9000–6000 BC; e.g. Goren and Goldberg 1991; Goren and Goring-Morris 2008). Since many indigenous tribes regularly used hot stones for cooking, it is plausible that the first application of lime as a binder was a matter of accident (Elsen 2006; Carran et al. 2012). Lime was originally used in plasters; the Romans firmly established the implementation as a binder for architectural purposes. Roman guidelines exist, providing instructions on the calcination procedure of either white limestone or marble (Cato in Hooper and Ash 1939; Vitruvius in Morgan 1914). Vitruvius recommended using limestones with relative high porosities for producing plasters and renders. The production of mortar became less well organised and more variable with the decline of the Roman Empire. Various materials (eggs, cheese, milk, blood) were added, but only a few mortars possessed hydraulic properties (Stark and Wicht 1998; Pavía and Caro 2008; Elsen et al.

✉ Janina Falkenberg
janina.falkenberg@rub.de

[1] Institute of Geology, Mineralogy and Geophysics, Ruhr-Universität Bochum, Universitätsstraße 150, 44801 Bochum, Germany

[2] Eichenallee 141, 33332 Gütersloh, Germany

2011; Carran et al. 2012). Mortar production changed in the eighteenth century; the hydraulic properties were increased by calcinating marly limestones at 950–1250 °C. Silicates of calcium and aluminium form at these high temperatures, allowing the lime to harden underwater (Boynton 1980; Ingham 2011). Consequently, lime-based mortars were thus quickly replaced by Portland cement as a binder. This mixture of pure limestones and clay or argillaceous earth, burnt at > 1500 °C, was first produced in 1824 (Carran et al. 2012).

The mortar production consists of three consecutive phases:

1. Calcination: $CaCO_3$ (carbonate-rich sedimentary rocks) + °C → CaO (= quicklime) + CO_2
2. Hydration/slaking: $CaO + H_2O \rightarrow Ca(OH)_2$ (= lime)
3. Carbonation: $Ca(OH)_2 + CO_2 \rightarrow CaCO_3 + H_2O$

In phase 1, the limestones are burned in kilns. The first kilns were probably simple pits, consisting of a central fire place and natural limestones piled up next to the walls of the pit. Alternatively, wood and limestones were arranged in alternating layers (Stark und Wicht 1998; Goren and Goring-Morris 2008). Clamp and flare kilns are the dominant types of kilns until the Industrial Revolution about 200 years ago. The charge of the clamp kiln, wood and limestone, was stacked in layers, which resulted in unevenly burnt lime. The Romans used mostly flare kilns, where wood and limestones were separated. The burning process here was more even (Dix 1982). The temperature reached in the calcination process and the duration of the burning process are still being discussed by archaeologists (e.g., Boynton 1980; Torraca 1995; Hughes et al. 2002; Goren and Goring-Morris 2008). A maximum temperature of 870 °C for less than 60 min has been observed in an experimental pit kiln (Goren and Goring-Morris 2008). The elaborate Roman guidelines suggest rather low, but stable temperatures for the calcination (Cato in Hooper and Ash 1939). The fuel is the second raw material important for fabricating mortar. The Romans used poplar for fierce heat and oak for slow burning (Dix 1982). Gradual heating results in a more successful calcination process than shock preheating. It produces highly reactive lime with low shrinkage, low density and high porosity (Boynton 1980; Kumar et al. 2007). The findings of lime lumps, which are caused by uneven burning, supply information about the burning temperature. Overburnt lime lumps indicate the temperature maximum reached during an individual burning procedure, while low burning temperatures are indicated by microfossil-bearing lime lumps (Elsen 2006). The size of the limestone boulders controls the necessary calcination temperature. Large limestone blocks require higher temperatures than smaller ones; particles with an underburnt centre and overburnt rim thus imply the usage of larger blocks (Boynton 1980).

The rate and speed of the exothermically reaction in phase 2 is related to the state of the lime and the amount of impurities (e.g., clay). Large amounts of impurities can block the pores and slow down the rate of hydration. Hydraulic lime requires a minimum of moisture, while non-hydraulic ones are rapidly slaked in contact with water at 90–100 °C. The slaking process can either produce dry lime powders or with excess water a lime putty. "Hot mixing" or "dry slaking" refers to a practice where damp aggregate is mixed with roughly crushed quicklime, causing the formation of large lime lumps (Dix 1982; Stark and Wicht 1998; Elsen 2006; Ingham 2011).

The 0.25–30-µm-long calcitic skeletons of calcareous nannofossils (Fig. 1) are the fossil ancestors of marine algae, which are very common in the modern oceans. The coccosphere (Fig. 1(a)), an extracellular skeleton formed by $CaCO_3$, is the characteristic feature of coccolithophores. This low Mg-calcitic shell consists of multiple plates (= coccoliths), each typically 1 to 10 µm across. The calcareous nannofossils include three morphologically different groups, two different types of coccoliths (hetero- and holococcoliths) and a third closely related group (nannoliths) with a deviating morphology (for details see Bown and Young 1998; Young and Henriksen 2003; Jordan 2009; Young 2020; Fig. 1(b)). Calcareous nannofossils first appeared 209 Ma ago in the Late Triassic (Gardin et al. 2012) and rapidly evolved ever since then, reaching highest diversities in the Late Cretaceous (100–66 Ma). When occurring in large numbers, calcareous nannofossils can be rock forming, resulting in the formation of chalks or limestones. These deposits are widespread throughout the Late Cretaceous of northern Europe, where they have been intensively mined in historic times. Their small size makes nannofossils an ideal tool for analysing archaeologically critical materials like colour paintings. Calcareous nannofossils have thus been described from, e.g., building stones, mortars and ceramics (von Salis 1995; Quinn and Day 2007; Quinn 2008; Lübke et al. 2018). Falkenberg et al. (2021) observed calcareous nannofossils in the lime binder of mortars of four medieval buildings in the Münsterland (northern Germany). The limebinders were carefully sampled, but the technique used does not exclude contamination from small lime lumps and aggregates. The microfossils successfully provided clear evidence for the provenance of the source rocks.

Archaeothermometry is another field, in which micro- and nannofossils may supply new information. To obtain an understanding of the morphological changes, which microfossils undergo during heating, experiments using unaltered raw material are crucial. Such data can then be used for reconstructing the temperatures reached during the calcination process. The preservation of the calcitic shells

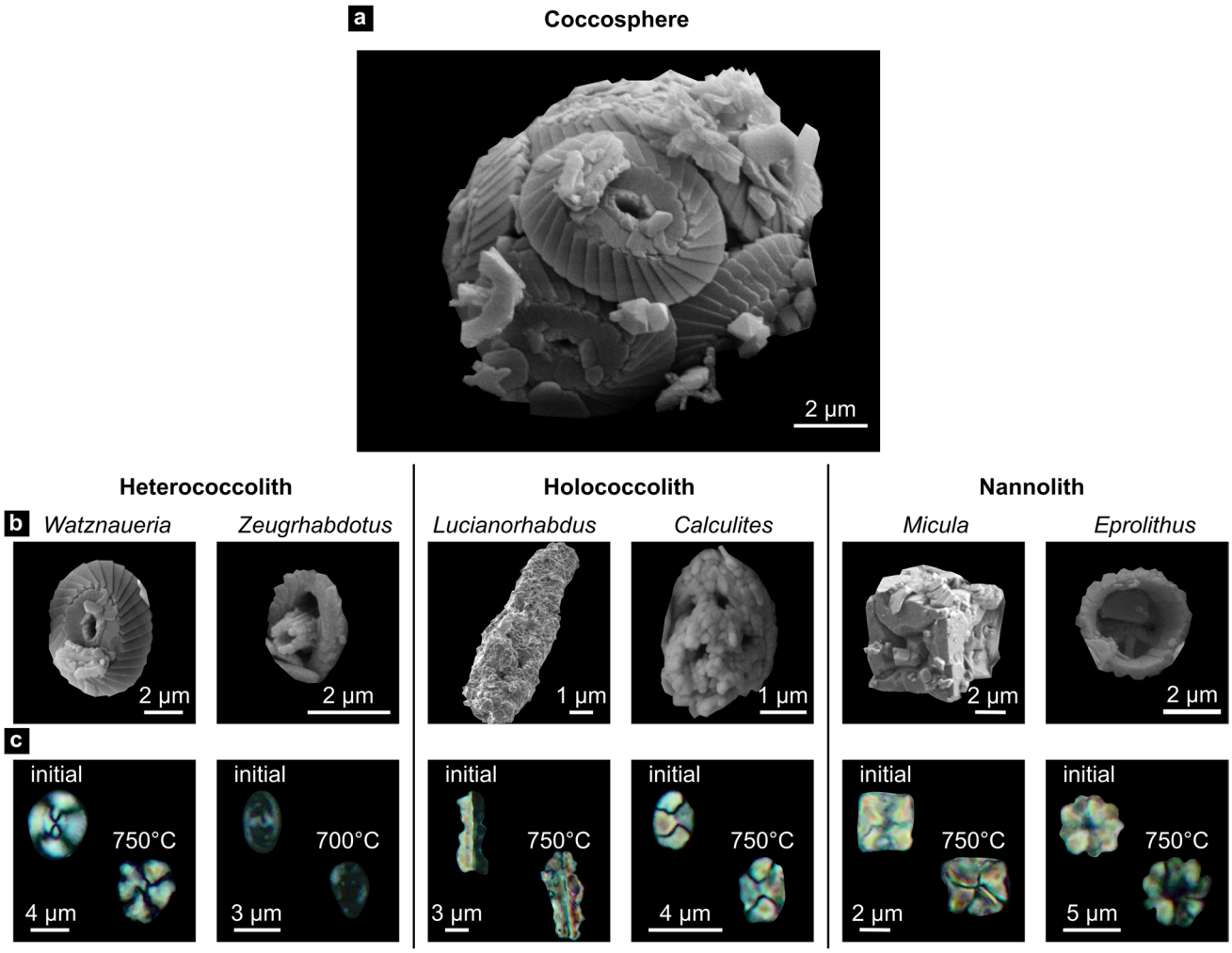

Fig. 1 (**a**) Scanning electron microscope image of a coccosphere (*Watznaueria barnesiae*) showing the individual coccoliths (modified after Falkenberg et al. 2021); (**b**) scanning electron microscope images of hetero-, holococcoliths and nannoliths, documenting their crystal size and form; (**c**) light microscope images of typical forms of nannofossils, showing the different preservation modes observed in the burning experiments. Top left: initial, unburnt coccolith. Bottom right: coccolith after burning (b, c modified after Falkenberg and Mutterlose 2022) (made using Inkscape).

of the nannofossils deteriorates during the calcination process, and they are completely destroyed at temperatures of around 850 °C. Additional factors which control the carbonate decomposition include the atmospheric conditions and impurities of the raw material (Webb and Krüger 1970; Quinn and Day 2007). Burning experiments of pristine, nannofossil-rich carbonates resulted in the recognition of four distinctive temperature phases. A second factor controlling the preservation is the $CaCO_3$ content (Falkenberg and Mutterlose 2022). The burning experiments also indicated that different crystal sizes and forms of the three morphological nannofossil groups result in different heat resistances when undergoing calcination from which heterococcoliths are the least heat-resistant group (Falkenberg and Mutterlose 2022; Fig. 1(c)).

Here, 33 mortar and mortar-based samples from 26 churches and historic buildings were studied along a geological transect of the Münsterland. By using ultra-thin sections, the calcareous nannofossil assemblages have been studied separately for each of the binder, lime lumps and aggregates in a given mortar. This part of the study is directed towards reconstructing the historic calcination processes used at different sites in the Münsterland.

In addition, 17 source rock samples from quarries were analysed. The relative abundances, preservation and diversity observed in the three mortar materials (binder, lime lump, aggregate) were compared to the unaltered assemblages of the corresponding source rock. By applying the results from the burning experiments, burning temperature ranges were obtained for the mortar samples. This new

method will thus contribute to a better understanding of the historic mortar production and the calcination process.

Geological setting

All historical buildings sampled here are located in the Münsterland or in adjoining areas (Fig. 2(a, b)). The Münsterland is confined by morphological ridges in the north (Teutoburg Forest) and in the east (Egge Ridge). Both ridges are formed by weathering-resistant sandstones of Early Cretaceous age. In the south, the Münsterland is bordered by the hill landscape of the Rhenish Massif, which is composed of sandstones and shales of Carboniferous age. In the west, Cenozoic siliciclastics crop out along the river Rhine. All four areas lack major limestone occurrences, while marine carbonate-rich sedimentary rocks of Cretaceous age are widespread in the subsurface of the Münsterland.

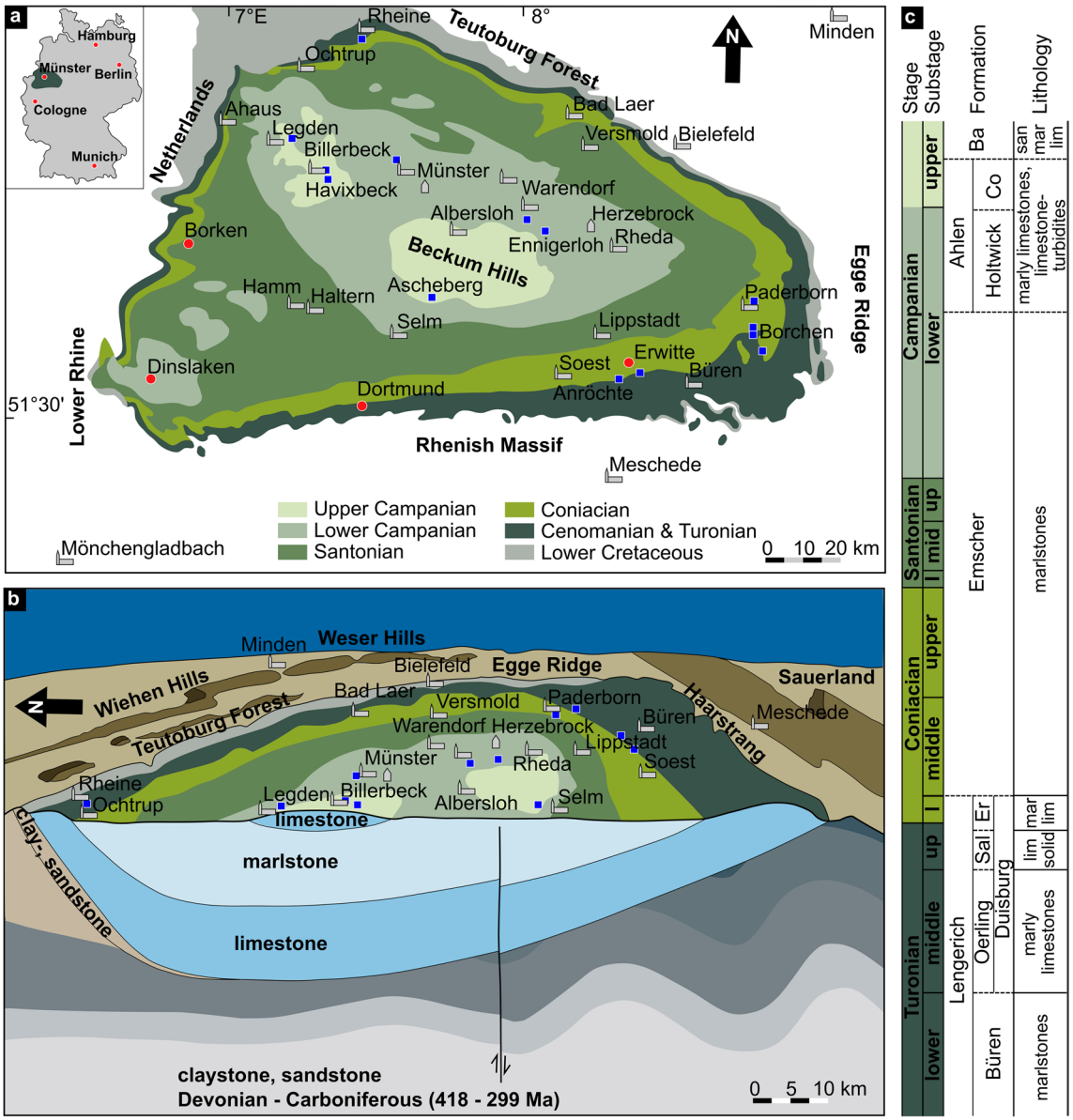

Fig. 2 Origin of the studied material. (**a**) Simplified geological map of the Münsterland Basin, Cenozoic removed. The studied churches and historic buildings are marked by symbols (church, church; historic building, house). Quarries and outcrops exposing the source rocks are shown as squares (modified after Hiss and Mutterlose 2010, Dölling et al. 2018 and Falkenberg et al. 2021); (**b**) cross section of the Münsterland Syncline showing the Cretaceous lime- and marlstones as well as the underlying Devonian and Carboniferous clay- and sandstones (modified after Hiss and Mutterlose 2010); (**c**) the important geological formations of the study area. l, lower; mid, middle; up, upper; Oerling, Oerlinghausen; Sal, Salder; Er, Erwitte; Co, Coesfeld; Ba, Baumberg; lim, limestones; mar, marly; san, sandy (modified after Falkenberg et al. 2021) (made using Inkscape)

The Albian-Campanian (113–72 Ma) carbonate-rich sedimentary sequences, exposed in the Münsterland, include marlstones, marly limestones and limestones. During the Cenomanian and Turonian, glauconitic-rich marlstones were deposited in the coastal areas of the southern Münsterland. Marlstones, marly limestones and limestones characterise the more distal part (central and northern Münsterland). An uplift of the Lower Saxony Basin in the north and of the Central Netherlands Basin in the west caused an accumulation of thick marlstone sequences (Coniacian-Santonian). Upper Santonian and Campanian sediments are sand- to glauconitic-rich marlstones and sandy limestones of a shallow marine facies (Fig. 2(c); Drozdzewski 1995; Hiss 1995; Voigt et al. 2008).

In the Palaeogene and Neogene marine sand- or clay-rich, partly glauconitic, sediments were deposited in the western part of the Münsterland (Skupin 1995). Quaternary sediments are of fluvial (sands, gravels), glacial (moraines, silts, sands, gravels) or aeolian origin (silts, sands; mostly angular quartz and feldspar). Common boulders in the moraines, having a Scandinavian provenance, are gneiss and granite (Skupin et al. 1993; Skupin and Staude 1995).

Material

A total of 33 samples (1–33) were collected from churches and historic buildings along a northwest-southeast transect of the Münsterland Syncline (Fig. 2(a, b); Table 1; Online Resource 1). Out of these, two samples were studied for more than one material, resulting in the analysis of 29 mortars, one render mortar, two renders, two plasters, one coloured coating and one chimney flank in total (Table 1). For the mortar and mortar-based samples, pieces of 1–2 cm^3 were taken (Fig. 3). The sampled materials cover approximately 1000 years of building history. The earliest material has been dated as 799 AD, the youngest goes back to the second half of the eighteenth century. The majority of the samples can be dated to the eleventh and twelfth century. To ensure that only original historic mortars were considered in this study, samples were taken from inner parts of the walls. The investigated parts were thoroughly screened for the presence of different mortar types to exclude younger repair or restoration.

A second set of source rock samples, about 5–10-mm^3-sized pieces of 17 source rocks (s1–s17), was collected from outcrops and quarries in the field (Fig. 2(a, b); Table 2; Online Resource 2). Each of the sampled quarries and outcrops exposes carbonate-rich sedimentary rocks (limestones, marly limestones) providing a potential source of the mortar used for the construction of the building nearby. The sources were identified based on the biostratigraphic analyses of the calcareous nannofossils of the mortar-based samples. The two sample sets, historic buildings and corresponding source rocks, allow a direct comparison of nannofossil assemblages from unaltered and mortar-based samples. This approach assigns a corresponding source rock to the historic sites studied here. More information of the sample locations, including the coordinates of the buildings (source: Google maps) and outcrops (source: TIM-online), can be found in Online Resources 1 and 2.

Methods

All mortar and source rock samples were first checked for their nannofossil content by using smear slides. The preparation technique is described in detail by Perch-Nielsen (1985). Materials from mortars, including binders, lime lumps and aggregates, were processed in this way.

Based on the nannofossil content observed in the smear slides of the mortars, 25 samples were selected for thin section analyses (Table 1). Due to the small size of the nannofossils, ultra-thin sections with a thickness of < 10 µm (Fig. 3) were made by Dr. Ulf Zinkernagel (Consulting Laboratory, Bochum). The ultra-thin sections were prepared following the standard procedure (e.g. Müller 1964; Tucker 1985; Miller 1988) with some modifications. Due to the intended reduced thickness of the preparations, the infeed rate during grinding must be carried out in closely spaced steps, which is extremely time consuming. This process ensures a weak surface roughness and protection of the objects from distortion. This preparation technique is near to the mechanical limits of accuracy for grinding equipment usually applied in practice.

Settling slides were produced from those source rock samples, where counting was possible in the ultra-thin sections of the corresponding mortar. Six settling slides were processed and analysed to obtain quantitative data. For details of the preparation technique, see Geisen et al. (1999).

Three source rocks samples (s14, s15, s17), showing low abundances of calcareous nannofossils, were counted in smear slides. For comparison, the calcareous nannofossils in the chimney flank were counted both in ultra-thin section and in smear slide; assemblages in the two corresponding source rocks (s4, s6) were also counted in a smear slide. Because of the low number of calcareous nannofossils in the Legden-Asbeck mortar sample, the nannofossils of the source rocks (s2, s3) were only counted in smear slides.

The ultra-thin sections (A-Y in Table 1) were analysed with an Olympus BH-2 cross-polarised immersion light microscope with magnifications of 25 × and 100 ×. Smear and settlings slides were studied with a magnification of 1250 ×, and five transects of each slide were examined. For the binder, at least five transects of each ultra-thin section were scanned for their nannofossil content; the same

Table 1 Origin of the studied mortar and mortar-based samples (1–33)

Building	Sample ID	Archaeological age	Location	Material	Thin section
Rheine, St. Dionysius	1	1510	Western tower, 1st floor	Mortar	A
	2	1520	Western tower, 1st floor	Mortar	B
Ochtrup-Langenhorst, St. Johannes	3	End of twelfth century	South-eastern tower, 2nd floor	Mortar	C
Ahaus-Wessum, St. Martinus	4	Fourteenth century	Western tower, 2nd floor	Mortar	D
Legden-Asbeck, St. Margareta	5	2nd half twelfth century	Western tower, 1st floor above gallery	Mortar	E
Billerbeck, St. Johann	6	Twelfth century, before 1234	Western tower, bell floor	Mortar	F
Bad Laer, St. Marien	7	Early Romanesque (eleventh century)	Western tower, 2nd floor	Mortar	-
Minden, Cathedral	8	1152	Westwork, observing platform	Mortar	-
Münster, Bergstraße 9	9	Seventh century	Ceiling, 1st floor	Render mortar	G
	10	2nd half eighteenth century	Room 6.05	Mortar, chimney flank	H
Münster-Nienberge, St. Sebastian	11	Romanesque	Western tower, bell floor	Plaster	I
Versmold, St. Petri	12	Romanesque, Gothic floors	Western tower, 3rd floor	Mortar	J
Albersloh-Sendenhorst, St. Ludgerus	13	2nd half thirteenth century	Southern column	Mortar	K
Bielefeld-Kirchdornberg, Peter's Church	14	1327	Western tower, bell floor	Mortar	-
Warendorf-Einen, St. Bartholomäus	15	Early thirteenth century	Western tower, bell floor	Mortar	-
Warendorf-Freckenhorst, St. Bonifatius	16	Late twelfth century	Attic floor, above choir	Mortar	L
	17	1116–1129		Mortar	M
Herzebrock-Clarholz, Provost's building	18	1715	Northern side of building	Render	N
Rheda-Wiedenbrück, Palace Rheda	19	Late Romanesque (thirteenth century)	Chapel tower, attic floor	Mortar	-
Selm-Cappenberg, St. Johannes	20	Twelfth century	Northern transept	Mortar	O
	21	Fifteenth century	Northern aisle	Mortar	P
Haltern-Flaesheim, St. Maria Magdalena	22	After 1166	Western tower, 2nd floor	Mortar	-
Hamm-Bossendorf, Heilig-Kreuz	23	Twelfth century	Western tower, 1st floor	Mortar	Q
Lippstadt-Benninghausen, St. Martin	24	Romanesque, twelfth century	Defence tower, 1st floor	Mortar	R
Soest, St. Patrokli	25	1180/90	Western tower, 2nd floor	Mortar	S
Paderborn, Cathedral	26	799 (IIa)	Western choir excavation	Mortar	T
	27	Gothic (1233–1241)	Collapsed intersection tower	Mortar, plaster, coloured coating	U
	28	Romanesque (IVb, 1084–1127)	Crypt	Mortar	V
Paderborn, Abdinghof Church	29	Eleventh century	Southern stair tower	Mortar	W
	30	Romanesque	Eastern choir	Render	X
Büren, St. Nikolaus	31	Late Romanesque (1220?)	Western tower, bell floor	Mortar	Y
Meschede, St. Walburga	32	Late Carolingian (around 860)	Crypt	Mortar	-
Mönchengladbach, town hall abbey	33	1723	Basement	Mortar	-

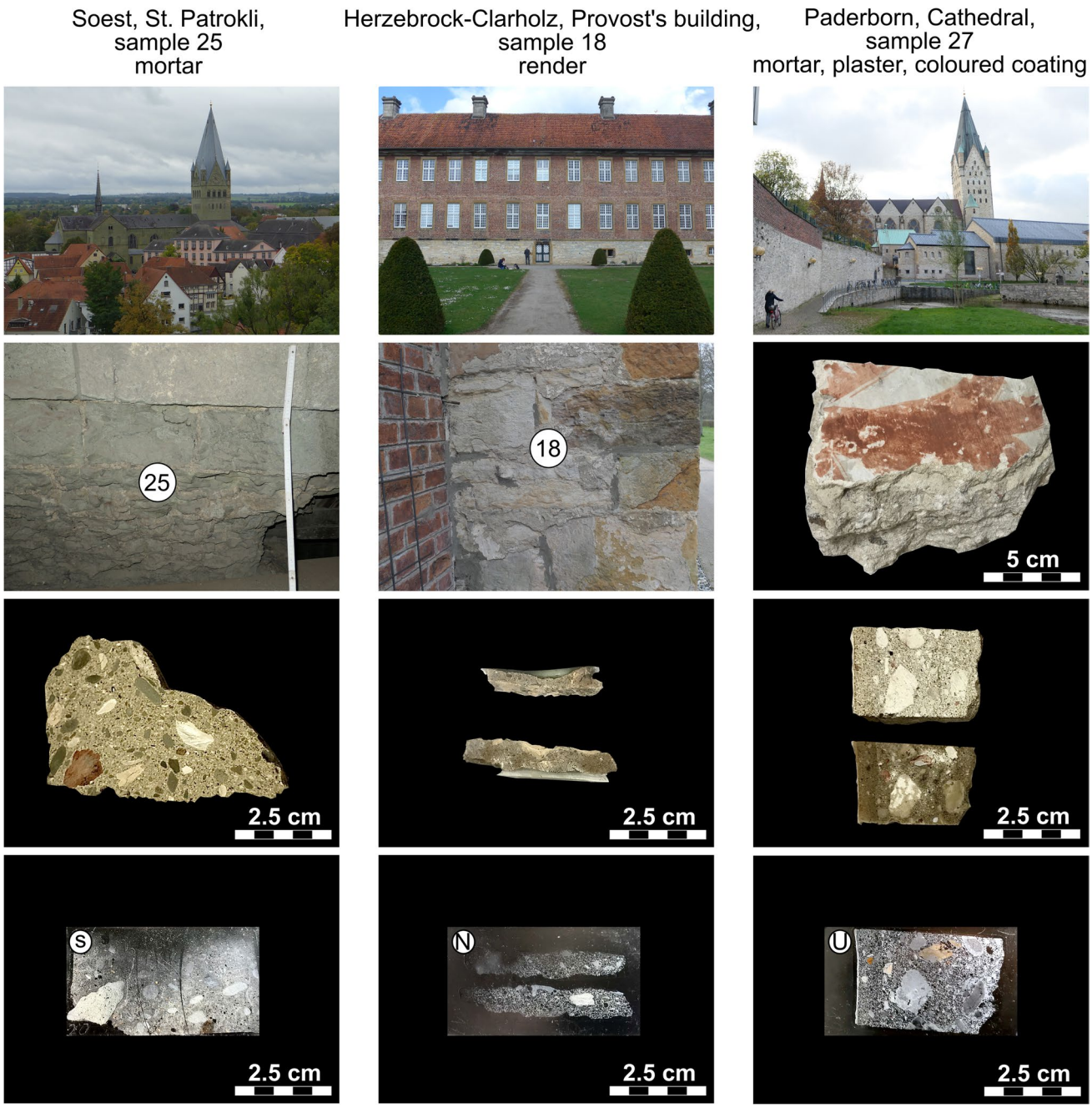

Fig. 3 Three selected study sites (Soest, Herzebrock-Clarholz, Paderborn) showing the historic building (top row), the sample location (second row), the individual sample (third row) and the ultra-thin section (bottom row) (made using Inkscape)

procedure was applied to the lime lumps and calcite-rich aggregates. At least 300 nannofossils were counted in each of the settling and smear slides in randomly chosen transects. Two randomly chosen traverses were checked for rare taxa. Calcareous nannofossils were counted in those ultra-thin sections, where binder, lime lumps or calcite-rich aggregates contained > 50 specimens. It was, however, not always possible to count 300 specimens. For larger lumps and aggregates, additional smear slides were produced. An Olympus SC100 camera was used for obtaining the LM (light microscope) images. All materials are stored in the Department of Geology, Mineralogy and Geophysics, Ruhr-Universität Bochum (Germany).

The biostratigraphic scheme used here recognises 21 biozones (UC0-20) and is based on Burnett (1998). A refined subdivision resulted in the recognition of 51 subzones (e.g. UC9a; Figs. 4 and 5). The preservational modes of the encountered calcareous nannofossils are as follows: good

Table 2 Origin of the studied source rock samples (s1–s17)

Location	Sample ID	Geological Age	Location outcrop	Sampling	Corresponding thin section
Rheine	s1	Middle Turonian	Rheine-Waldhügel	Lower Lengerich Formation	A
Legden-Asbeck	s2	Late Campanian	Schöppingen	Coesfeld Formation	E
	s3	Early Campanian	Schöppingen	Holtwick Formation	
Billerbeck	s4	Late Campanian	Billerbeck	Baumberge Formation	F
Münster	s5	Early Campanian	Münster-Nienberge	Ahlen Formation	H
Albersloh-Sendenhorst	s6	Late Campanian	Havixbeck	Baumberge Formation	K
Warendorf-Freckenhorst	s7	Early Campanian	North of "Schulze Niehues"	Ahlen Formation	L
	s8	Early Campanian	Brummort	Ahlen Formation	M
Herzebrock-Clarholz	s9	Early Campanian	Ennigerloh-Ostenfelde	Ahlen Formation	N
Selm-Cappenberg	s10	Early Campanian	Ascheberg-Herbern	Holtwick Formation	O
Soest/Büren	s11	Middle Turonian	Rüthen-Westereiden	Oerlinghausen Formation	S
	s12	Late Turonian	Anröchte-Klieve	Duisburg Formation	S, Y
	s13	Early Coniacian	Rüthen-Westereiden	Erwitte Formation	
Paderborn	s14	Late Turonian	Borchen-Kirchborchen	Lower Salder Formation	T, U
	s15	Late Turonian	Borchen-Nordborchen	Upper Salder-Formation	
	s16	Early Coniacian	Sample from crypt, original raw material from the Meinwerk quarry, Kötterhagen	Erwitte Formation	W
	s17	Middle Turonian	Borchen-Etteln	Upper Oerlinghausen Formation	X

(minor fragmentation and etching), good-moderate (minor to moderate fragmentation and etching), moderate (moderate fragmentation and etching), moderate-poor (moderate to major fragmentation and etching) and poor (major fragmentation and etching). For details, see Roth and Thierstein (1972) and Roth (1983). The Shannon Index, a measure for recording heterogeneity and species richness, was used for quantifying the diversity (Shannon and Weaver 1949). Very diverse assemblages show a high Shannon Index, less diverse ones have a lower index.

Results

Ultra-thin section descriptions

Binder, aggregates, additives

All 25 ultra-thin section samples studied here have a cryptocrystalline lime-based binder (Table 3). In 23 ultra-thin sections, a few isolated larger crystals of up to 50 µm, rarely up to 400 µm in size, have been observed inside a fine-grained matrix.

The aggregates are subrounded to subangular and are generally moderately well-graded to well graded. In most samples, aggregate sizes vary from 10 µm to a few millimetres. The dominant mineralogical phase present in all samples is quartz. Plagioclase, alkali feldspar and pyroxene were observed in most samples. Rarer minerals include mica, biotite, hematite, glauconite and opaque minerals. Common rock fragments include sand-, silt- and claystones, quartzites as well as marl- and limestones. Seldomly observed rock fragments are gneiss, granites and schists (Table 3).

All samples except for samples 10, 16 and 25 contain additives; the most common are wood or charcoal. Ceramic fragments, organic material and hairs have also been observed (Table 3). A more detailed list is documented in Online Resource 3.

Lime lumps

Lime lumps, binder-derived particles, have been found in all but one sample (9 — Münster; Table 3). Lumps, which are resembling the binder but do not show aggregates, have been observed in all samples with lime lumps. These lumps are only visible due to the presence of microcracks, a densification or a brighter birefringence than the binder. Common are further lime lumps containing fossils (e.g. foraminifera, bivalve shells, echinoderm fragments) or sedimentary structures. Only four samples are barren of these types of lumps (Table 3). Some lime lumps yield calcite crystals bigger than those observed in the binder (microcrystalline, between a few µm and a few 100 µm) and do not show aggregates. A more detailed description is given in Online Resource 3.

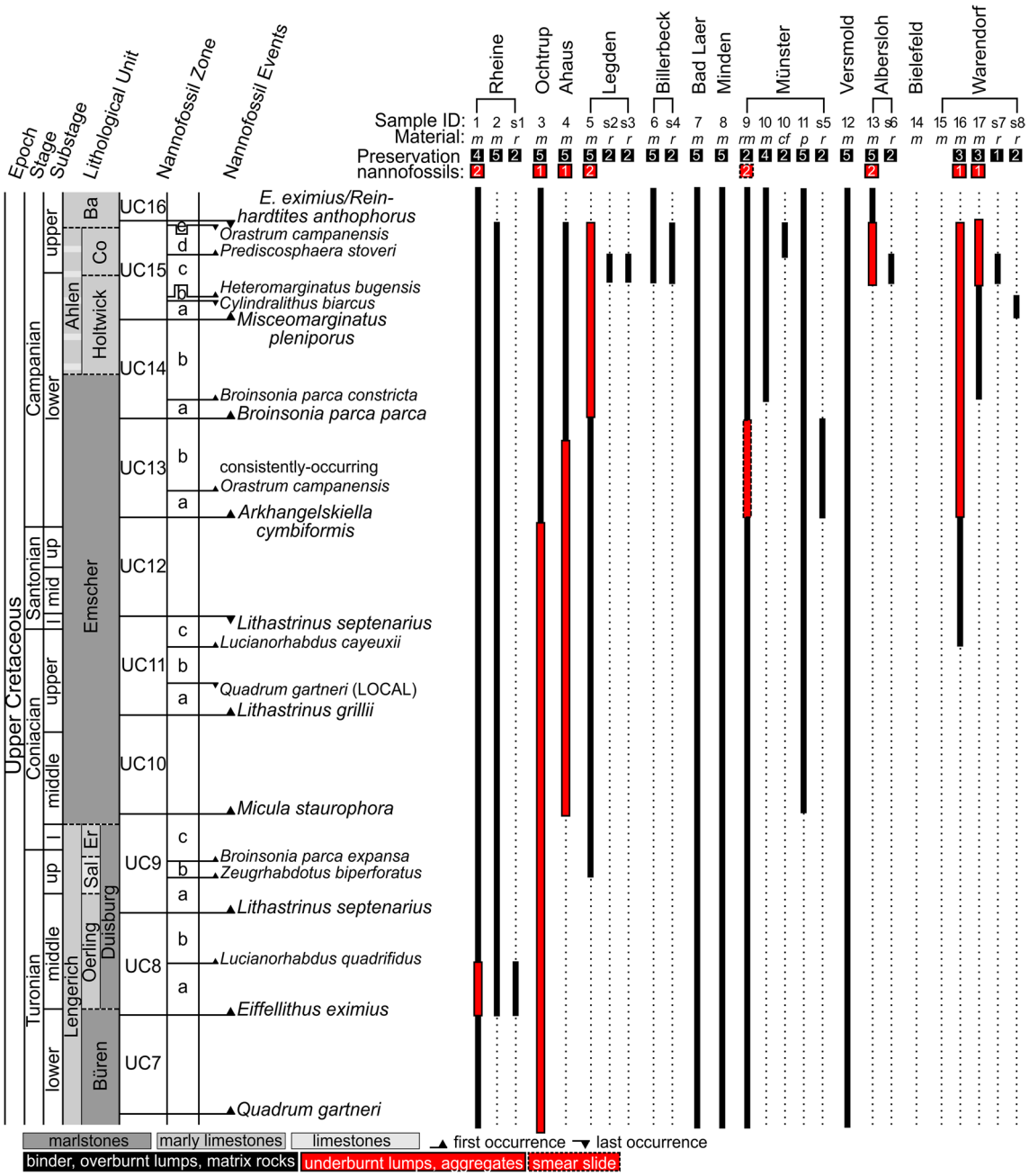

Fig. 4 Stratigraphic range of mortar, mortar-based and corresponding source rock samples from 12 sites in the northern part of the Münsterland and adjoining areas (Rheine-Warendorf), based on calcareous nannofossils in the binder, overburnt lime lumps, matrix of the source rocks (bar) and underburnt lime lump, aggregate (bar with frame). The preservation of the calcareous nannofossils is given from the binder, overburnt lime lumps, matrix of the source rocks (square) and underburnt lime lump, aggregate (square with frame). l, lower; mid, middle; up, upper; Oerling, Oerlinghausen; Sal, Salder; Er, Erwitte; Co, Coesfeld; Ba, Baumberg; sX, source rock samples; m, mortar; r, rock; rm, render mortar; cf, chimney flank; p, plaster; for the preservation: 1, good; 2, good-moderate; 3, moderate; 4, moderate-poor; 5, poor (made using Inkscape)

Calcareous nannofossils

Age ranges and preservation

Four of the 33 mortar and mortar-based samples are barren of calcareous nannofossils (Figs. 4 and 5). Stratigraphically long-ranging species like *Watznaueria barnesiae* (Fig. 6) were observed in the binders of 23 samples, allowing rather vague age assignments (Jurassic to Cretaceous or Late Cretaceous; Figs. 4 and 5). A more precise age range can be given for the lime binder of samples 6 (Billerbeck), 9 (Münster, smear slide only), 10 (Münster), 13

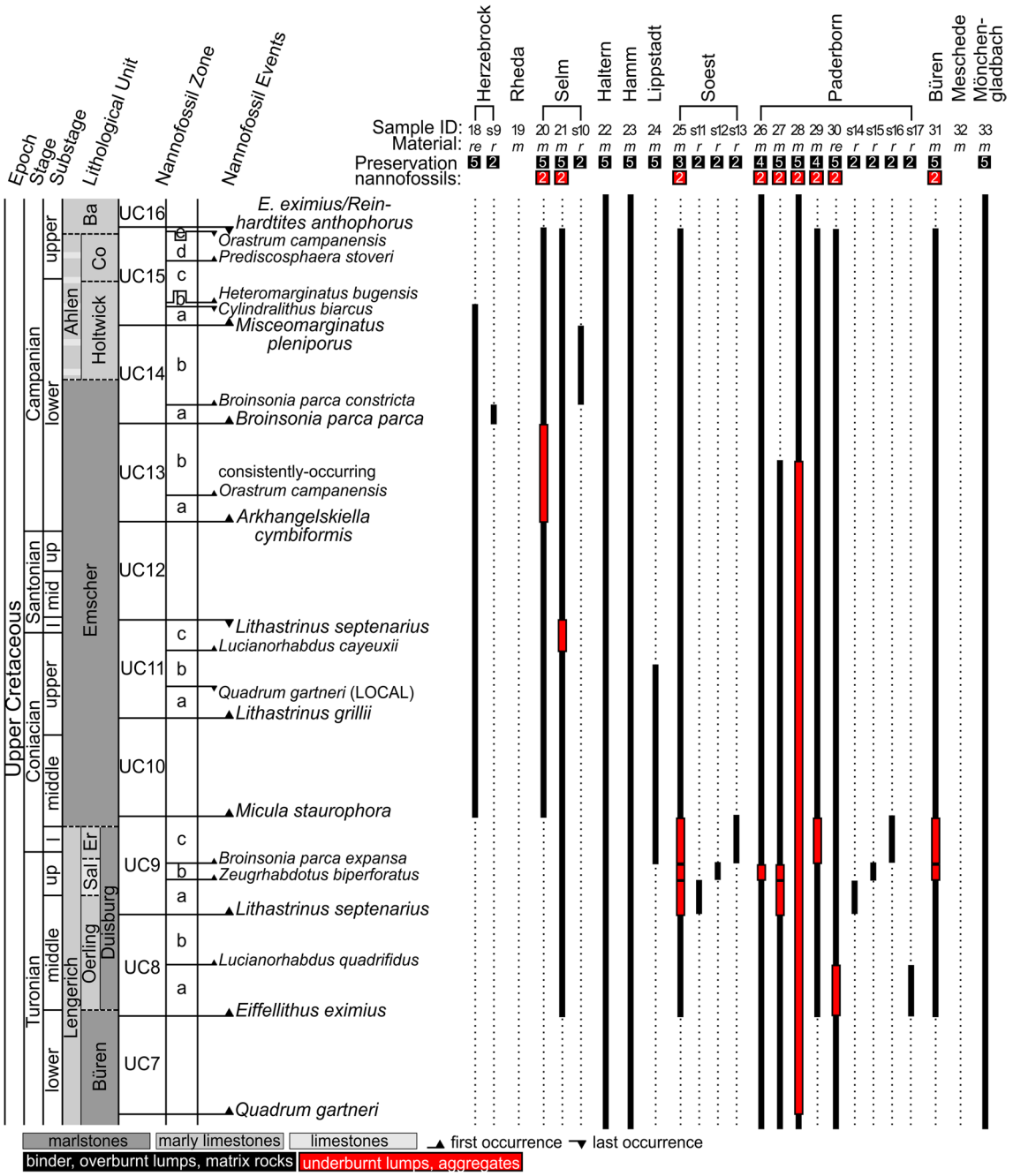

Fig. 5 Stratigraphic range of mortar, mortar-based and corresponding source rock samples from 11 sites in the southern part of the Münsterland and adjoining areas (Herzebrock-Mönchengladbach), based on calcareous nannofossils in the binder, overburnt lime lumps, matrix of the source rocks (bar) and underburnt lime lump, aggregate (bar with frame). The preservation of the calcareous nannofossils is given from the binder, overburnt lime lumps, matrix of the source rocks (square) and underburnt lime lump, aggregate (square with frame). l, lower; mid, middle; up, upper; Oerling, Oerlinghausen; Sal, Salder; Er, Erwitte; Co, Coesfeld; Ba, Baumberg; sX, source rock samples; m, mortar; r, rock; re, render; for the preservation: 1, good; 2, good-moderate; 3, moderate; 4, moderate-poor; 5, poor (made using Inkscape)

(Albersloh-Sendenhorst), 17 (Warendorf-Freckenhorst) and 24 (Lippstadt-Benninghausen; Figs. 4 and 5).

The calcareous nannofossils encountered in the underburnt lime lumps and aggregates provide more precise biostratigraphic age ranges for 16 of the 25 ultra-thin sections. Nine of these more precisely dated samples have been attributed to a specific biozone (samples 1 — Rheine; 20 and 21 — Selm-Cappenberg; 25 — Soest; 26, 27, 29, 30

Table 3 Petrographic characteristics of the studied mortar and mortar-based samples observed in the ultra-thin sections. *Qz* quartz, *Pl* plagioclase, *Px* pyroxene, *Bt* biotite, *Afs* alkali-feldspar, *Glt* glauconite, *Hem* hematite, *Mca* mica, *Op* opaque mineral, *Qtzt* quartzite, *Ss* sandstone, *Sltst* siltstone, *Clst* claystone, *Mrl* marlstone, *Ls* limestone, *sdy* sandy, *Gnss* gneiss, *Gt* granite, *Sch* schist, *Ob* overburnt/well calcined, *Ub* underburnt, *Agg* aggregate

Building	Thin section	Binder	Aggregate		Additives	Lime lumps
			Mineralogical phases	Rock fragments		
Rheine, St. Dionysius	A	Lime	Qz, Pl, Px, Bt	Sltst	Wood	Ob, Ub/Agg
	B	Lime	Qz, Pl, Afs, Px, Glt, Bt, Hem	Sltst, Clst, Mrl	Wood, ceramic	Ob, Ub, Agg
Ochtrup-Langenhorst, St. Johannes	C	Lime	Qz, Pl, Afs, Px, Hem, Bt, Mca	Sltst, Ss, Clst	Wood, charcoal	Ob, Ub/Agg
Ahaus-Wessum, St. Martinus	D	Lime	Qz, Pl, Afs, Hem, Px	Ss, Clst	Hair, wood	Ob, Ub/Agg
Legden-Asbeck, St. Margareta	E	Lime	Qz, Pl, Afs, Glt, Px, Hem, Op	Ss, Qtzt, Clst, Mrl, Gnss	Charcoal, wood, hair	Ob, Ub/Agg
Billerbeck, St. Johann	F	Lime	Qz, Pl, Afs, Hem, Glt, Op	Ss, Clst, Qtzt	Wood, organic material	Ob
Münster, Bergstraße 9	G	Lime	Qz, Pl, Glt, Op, Hem, Px, Mca	Clst, Mrl, Sltst, Ss, Qtzt	Wood, charcoal	-
	H	Lime	Qz, Glt, Pl, Afs, Op, Px, Hem	Clst, Qtzt, Ss, Mrl	-	Ob, Ub/Agg
Münster-Nienberge, St. Sebastian	I	Lime	Qz, Pl, Afs, Glt, Hem, Bt, Px	Sltst, Ss, Clst, Mrl	Wood, hair	Ob
Versmold, St. Petri	J	Lime	Qz, Pl, Afs, Px, Hem	Ss, Qtzt, Clst	Charcoal	Ob
Albersloh-Sendenhorst, St. Ludgerus	K	Lime	Qz, Pl, Afs, Glt, Hem, Px, Mca, Op	Ss, Gt, Qtzt, Sltst, Clst	Ceramic	Ob, Ub/Agg
Warendorf-Freckenhorst, St. Bonifatius	L	Lime	Qz, Pl, Px, Hem, Op, Bt	Ss, Sltst, Clst	-	Ob, Ub/Agg
	M	Lime	Qz, Pl, Glt, Hem, Px, Op	Sltst, Clst	Wood	Ob, Ub/Agg
Herzebrock-Clarholz, Provost's building	N, mortar	Lime	Qz, Pl, Afs, Px, Op, Hem, Mca	Clst, Ss, Qtzt	Wood, hair	Ob, Ub
	N, render	Lime	Qz, Px	-	-	Ob
Selm-Cappenberg, St. Johannes	O	Lime	Qz, Pl, Afs, Hem, Px, Glt, Op	Clst, Sltst, Ss, sdy Ls	Wood, charcoal	Ob, Ub/Agg
	P	Lime	Qz, Pl, Afs, Glt, Hem, Px, Op	Ss, Sltst, Clst, sdy Ls	Ceramic	Ob
Hamm-Bossendorf, Heilig-Kreuz	Q	Lime	Qz, Pl, Afs, Glt, Hem, Op, Px, Mca	Clst, Sltst	Wood	Ob, Ub/Agg
Lippstadt-Benninghausen, St. Martin	R	Lime	Qz, Pl, Hem	Ss, Qtzt	Wood	Ob, Ub/Agg
Soest, St. Patrokli	S	Lime	Qz, Hem, Glt	Ls, Mrl, Clst, Ss, Sch	-	Ob, Ub, Agg
Paderborn, Cathedral	T	Lime	Qz, Pl	Sltst, Ls	Charcoal	Ob, Ub, Agg
	U, mortar	Lime	Qz, Pl, Afs, Hem, Px, Mca	Ls, Qtzt, Clst, sdy Ls, Mrl	Wood	Ob, Agg
	U, plaster	Lime	Qz	-	-	Ob
	U, coloured coating	Lime, fired clay minerals	-	-	-	-
	V	Lime	Qz, Px, Mca	Clst, Mrl, Ss	Ceramic	Ob, Ub, Agg
Paderborn, Abdinghof Church	W	Lime	Qtz, Pl	Mrl, Clst, Sltst	Charcoal, ceramic	Ob, Ub, Agg
	X, mortar	Lime	Qz, Pl, Afs, Px, Hem	Sltst, Mrl, Clst	Ceramic	Ob, Ub/Agg
	X, middle layer	Lime	Qz	-	-	-
	X, outer layer	Lime	Qz, Hem, Op	-	-	Ob
Büren, St. Nikolaus	Y	Lime	Qz, Hem, Glt, Op	Ls, Ss, Mrl, Sltst, Clst	Wood, charcoal	Ob, Ub/Agg

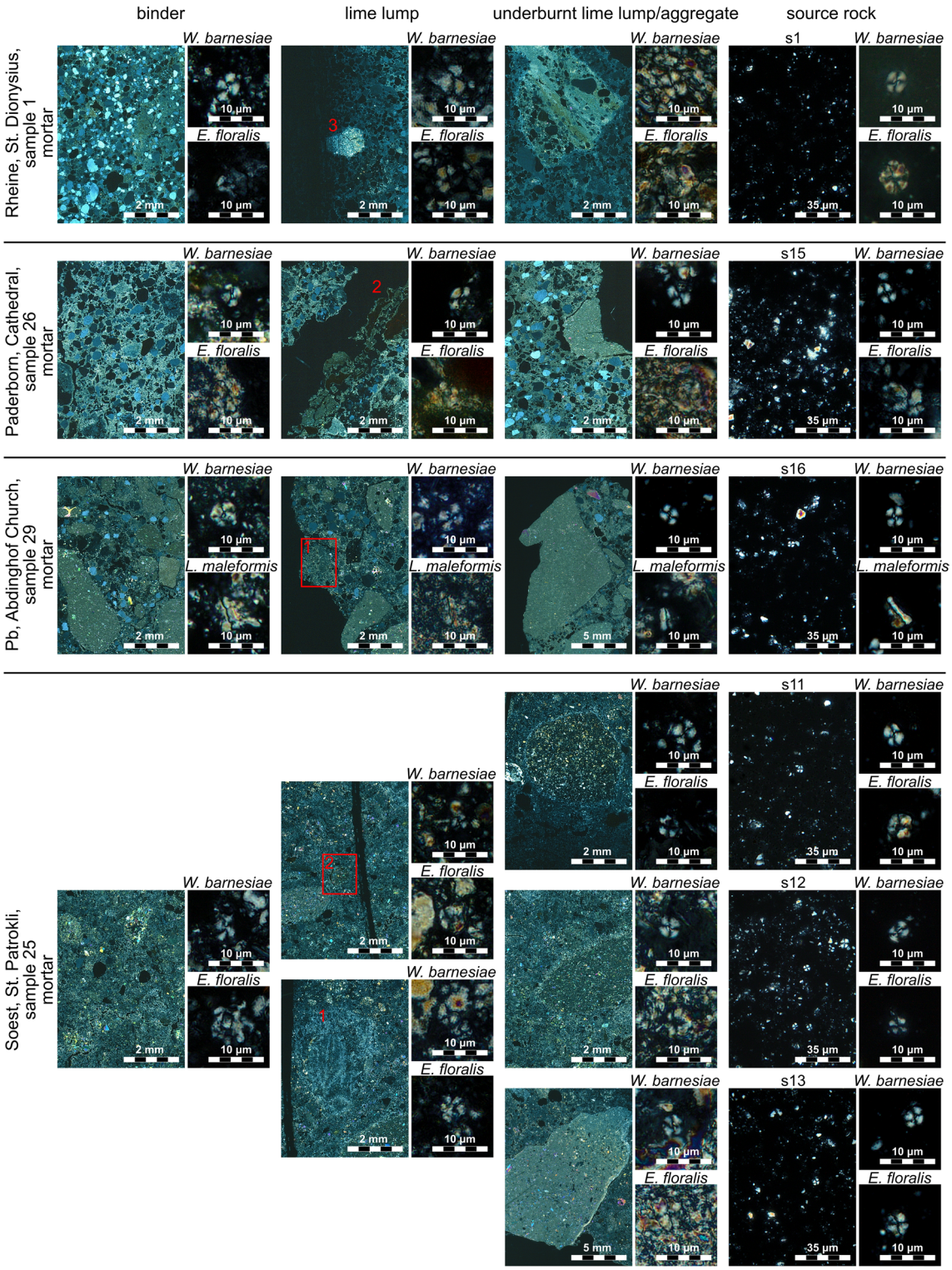

Fig. 6 Mortar samples from four different historic sites on the y-axis (Rheine, Paderborn Cathedral, Paderborn Abdinghof Church, Soest), showing the preservation of three nannofossil species on the *x*-axis (*Watznaueria barnesiae* — heterococcolith, *Lucianorhabdus maleformis* — holococcolith, *Eprolithus floralis* — nannolith) under crossed nicols. The nannofossils are from the binder, lime lumps, underburnt lime lumps/aggregates and correlating source rocks (samples: sX, see Table 2). The ultra-thin section images and the overview smear slide images were taken under crossed nicols. In two images, the rectangle shows the examined material. Pb, Paderborn; 1, lime lump only evident due to the presence of microcracks, a densification or a brighter birefringence than the binder; 2, lime lump with overburnt rim or burnt parts; 3, lime lump with crack and partly bigger calcite crystals than binder (made using Inkscape)

— Paderborn; 31 — Büren; Figs. 4 and 5). In addition, two of these 16 samples were attributed to a stratigraphically slightly broader UC15c-e interval (samples 13 — Albersloh-Sendenhorst; 17 — Warendorf-Freckenhorst; Fig. 4). In three of these samples (samples 25 — Soest; 27 — Paderborn; 31 — Büren), the co-occurring underburnt lime lumps and aggregates have been assigned to different biozones (Fig. 5). The nannofossils observed in the chimney flank provide a late Campanian age (UC 15d, Baumberge Formation; Fig. 4.) In all 17 source rocks studied here, the calcareous nannofossils allow a precise assignment to a specific biozone (Figs. 4 and 5).

The preservation of the calcareous nannofossils in the binder is often poor or moderate-poor (Figs. 4, 5 and 6). Exceptions are seen in the binder of the render mortar (sample 9 — Münster) with a good-moderate preservation. The mortar samples from Warendorf-Freckenhorst (samples 16 and 17; Fig. 4) and from Soest (sample 25; Figs. 5 and 6) show a moderate preservation of the calcareous nannofossils in the binder. In the underburnt lime lumps, aggregates and in the chimney flank the calcareous nannofossils have a good-moderate preservation (Figs. 4, 5 and 6). Only four samples show a good preservation of the nannofossils in the underburnt lime lumps/aggregates (Fig. 4). The preservation of the calcareous nannofossils in the source rocks is generally good-moderate; a good preservation was only observed in sample s7 (Warendorf-Freckenhorst). Details of the calcareous nannofossil content and preservation are documented in Online Resource 4.

Diversity and relative abundances

The binders of the samples show generally very low diversities; a maximum of 13 species has been encountered in samples 16 and 17. Most common taxa include *W. barnesiae*, *Eprolithus floralis* (Fig. 6) and *Tranolithus orionatus*. Counting in the binder was only possible in two mortar samples, which also show higher diversities. In sample 25 (Soest), 21 species and 112 specimens have been counted; in sample 29 (Paderborn), 14 species and 94 specimens (Online Resource 4). Diversities observed in the counted lime lumps and aggregates vary between 20 and 52 species, in the corresponding source rocks between 28 and 58 species (Fig. 7). The Shannon Index of these assemblages ranges between 1.9 and 3.0 for the underburnt lime lumps/aggregates and between 1.9 and 3.3 for the source rocks.

The most abundant genus in all samples is *Watznaueria* with 11.0% in the chimney flank and 69.1% in the binder of sample 29 (Fig. 7). Other common genera are *Prediscosphaera* (1.1% in the binder of sample 29, 36.1% in the chimney flank), *Eiffellithus* (1.5% in a lime lump/aggregate of sample 26, 17.0% in lime lump/aggregate 3 of sample 25) and *T. orionatus* (1.6% in s6, 18.0% in a lime lump/aggregate of sample 5; Fig. 7; Online Resource 4). The small heterococcolith genus *Biscutum* is rare (< 10%). Holococcoliths and nannoliths are also rare (< 10%), except for *Lucianorhabdus* and *Eprolithus* in sample 25 and *Micula* in s6 and s10. The relative abundances in the binder/lime lump/aggregate and the corresponding source rock are in general rather similar, but maximum differences of up to 20% have been observed (Fig. 7; Online Resource 4).

Discussion

Provenance analysis

Aggregates, additives

The common findings of subrounded-subangular quartz, feldspar, sand-, silt- and claystone as aggregates argue for the usage of Cenozoic fluvial and glacial deposits, which have a widespread occurrence in the Münsterland. Kühn (1986) and Lobbedey (1986) have documented the presence of quartz fragments in the mortars of the Paderborn Cathedral, suggesting glacial deposits from the Senne as a source. The mineral glauconite was observed in 13 mortar and mortar-based samples (Table 3), all of which are characterised by glauconite-rich carbonates cropping out nearby. The presence of gneiss, granite and schist as aggregates in Legden-Asbeck (sample 5), Albersloh-Sendenhorst (sample 13) and Soest (sample 25; Table 3) suggests the usage of glacial moraine material. This Scandinavian-derived material is a common component of glacial deposits occurring in this part of the Münsterland (Skupin et al. 1993).

Wood and charcoal fragments, found here in 18 mortar and mortar-based samples, are often observed in historic mortars and are probably remnants of the burning process, since wood was used as fuel (Elsen 2006). Hairs, well known from other historic sites, were found in four mortar samples, presumably intended to increase the tensile strength (Elsen 2006). Ceramic fragments are common mortar additives in Europe, particularly in the Mediterranean area, where they were used as pozzolans to improve the hydraulic properties (Elsen 2006), which could explain the findings here. Fragments of bricks were observed in the mortars of Paderborn by Kühn (1986), who postulated that building waste was used as aggregates/additives for mortar production.

Binder, lime lumps, carbonate-rich aggregates

Mortar samples from five sites (Rheine, Bad Laer, Versmold, Haltern-Flaesheim, Hamm-Bossendorf) only yield long-ranging species like *W. barnesiae*. A detailed provenance

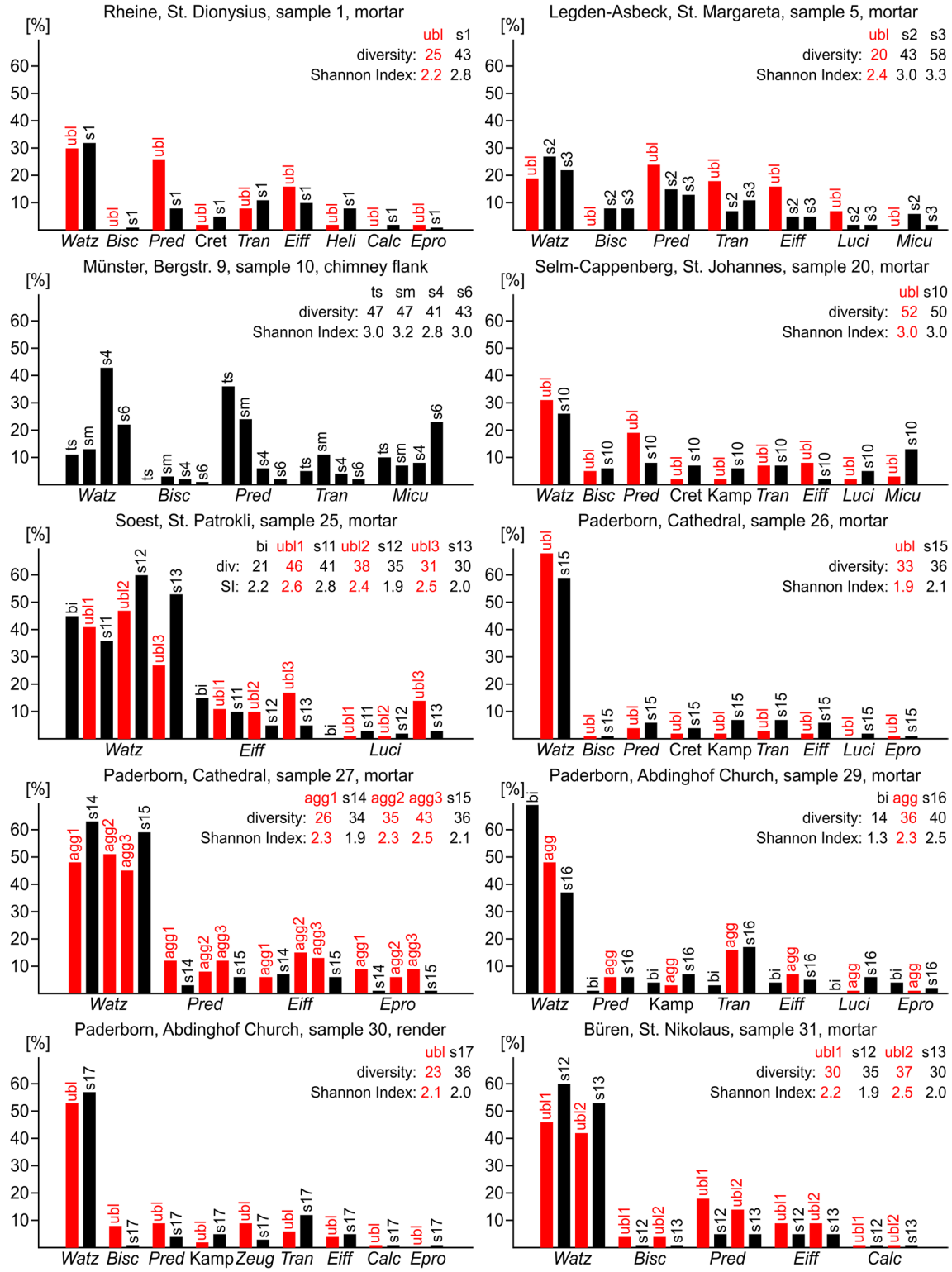

Fig. 7 Comparison of the relative abundances of calcareous nannofossil genera and species from components of the mortar (binder, lime lump, aggregate) and correlating source rocks (samples sX, see Table 2) of nine samples. For the chimney flank sample, the relative abundances are compared from the ultra-thin section, smear slide analysis and two possible source rocks. ubl, underburnt lime lump/aggregate; agg, aggregate/underburnt lime lump; ts, ultra-thin section; sm, smear slide; bi, binder; div, diversity; SI, Shannon Index; *Watz*, *Watznaueria* spp.; *Bisc*, *Biscutum* spp.; *Pred*, *Prediscosphaera* spp.; Cret, Cretarhabdaceae; *Tran*, *Tranolithus orionatus*; *Eiff*, *Eiffellithus* spp.; *Heli*, *Helicolithus* spp.; *Calc*, *Calculites* spp.; *Epro*, *Eprolithus* spp.; *Luci*, *Lucianorhabudus* spp.; *Micu*, *Micula* spp.; Kamp, Kamptneriaceae; *Zeug*, *Zeugrhabdotus* spp. (made using Inkscape)

analysis of these mortars is not possible; the Late Cretaceous sedimentary rocks of the entire Münsterland may have provided the necessary $CaCO_3$ (Figs. 4 and 5). For Minden (sample 8), the finding of *W. barnesiae* argues for the use of upper Jurassic limestones, which crop out in the vicinity (Grupe 1933). The findings of calcareous nannofossils in Mönchengladbach (sample 33) document that the source rocks must have been transported in this case over a distance of at least 70–90 km from the Aachen-Maastricht region. This is geologically the closest area were nannofossil yielding limestones crop out (Klostermann et al. 1990; Fig. 2).

In ten localities (Rheine, Ochtrup-Langenhorst, Legden-Asbeck, Billerbeck, Münster-Nienberge, Warendorf-Freckenhorst, Lippstadt-Benninghausen, Soest, Büren, Paderborn; Fig. 8), the raw material is of local origin (< 5 km distance). In mortar sample 1 of Rheine, the builders unexpectedly used marly limestones of the lower Lengerich Formation from Rheine-Waldhügel (s1; distance: 2 km; Fig. 8), though Cenomanian limestones crop out near the church. Lime kilns, burning Cenomanian limestones, are also historically documented in Rheine (Kommende Steinfurt 1686–1722). In this case, several rock sources may have been mined for supplying the mortar. For Ochtrup-Langenhorst (mortar sample 3; Fig. 4), a likely source are rocks from the Bilker Berg quarry (distance: 6 km) or the Weiner/Seller Esch quarries (distance: 1 km/5 km; Fig. 8). The latter were also used as building stones in the masonry (Kaplan 2009). The nannofossils from Legden-Asbeck (mortar sample 5; Fig. 4) suggest three potential source rocks. Either the Holtwick Formation or the Coesfeld Formation, both within a distance of 2 km of the church, or the Baumberge Formation (distance: 10 km; Fig. 8) provided the carbonate for the burning process. The building stones of the masonry come in this case from the Baumberge Formation (Kaplan 2009). The mortar samples of Soest (sample 25) and Büren (sample 31) document that for both sites, the mortar was provided from more than one source rock. The mortars of Soest and Büren indicate three resp. two different source rocks (Fig. 5). Soest green sandstone was used as a building stone in the masonry in Soest; Rüthen green sandstone was applied for the masonry in Büren (Kaplan 2009). It is quite likely that in both cases, the carbonates under- and overlying the green sandstone unit have been burnt jointly and used as mortar source. Paderborn (samples 26, 29 and 30; Fig. 5) shows different source rocks for each of the three mortar and mortar-based samples. The Erwitte Formation, cropping out directly in Paderborn (s16), the Salder Formation, exposed in Borchen-Kirchborchen (s14, distance: 5 km) and Borchen-Nordborchen (s15, distance: 4 km) and the Oerlinghausen Formation in Borchen-Etteln (s17, distance: 6 km) were all used for the mortar production (Fig. 8). In one mortar sample (27; Fig. 5), two source rocks have been used. These observations are supported by previous studies which document the application of rocks from all three formations for mortar production (Falkenberg et al. 2021) and for building stones (Kaplan 2009; Lübke et al. 2018). Potential explanations are seen in a locally limited availability of wood or in the ownership of land and quarries.

For three sites (Münster, Herzebrock-Clarholz, Selm-Cappenberg), the source rocks were transported over a short distance of 5–10 km. The limestones used in Münster most likely came from Altenberge-Hohenhorst or Münster-Nienberge. One source rock (s5) was taken from a limestone turbidite of the Ahlen Formation in Münster-Nienberge (distance: 5 km; Fig. 8). The historic quarries in Altenberge-Hohenhorst (distance: 8 km) have been filled in; sampling was thus impossible. Source rock sample s5 and render mortar sample 9 have the same stratigraphic age.

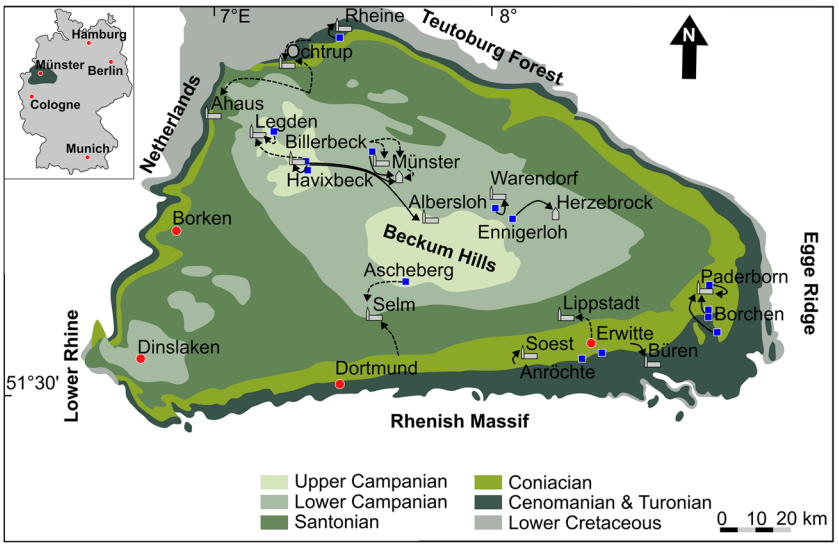

Fig. 8 Provenance analysis of the studied samples. Simplified geological map of the Münsterland Basin, Cenozoic removed. The churches and historic buildings are marked by symbols (church, church; historic building, house). Quarries and outcrops exposing the source rocks are shown as squares. Well-documented source rock areas are indicated by a solid line, questionable ones by a dashed line (modified after Hiss and Mutterlose 2010, Dölling et al. 2018 and Falkenberg et al. 2021) (made using Inkscape)

Mortar sample 10 indicates a younger age; potential source rocks either come from Altenberge-Hohenhorst (Fig. 8) or the Baumberge Formation. Another possibility is that source rocks derive from a quarry directly in Münster, which also supplied the building material for the Cathedral in Münster (Wegner 1927; Kaplan 2009). The mortar samples from Selm-Cappenberg (samples 20 and 21; Fig. 5) were transported from outcrops over 8 km from Ascheberg-Herbern (s10, Holtwick Formation) and from Bergkamen (Erwitte Formation) over a distance of 10 km (Fig. 8). The building stones of the masonry are in contrast provided from quarries directly in Cappenberg (Kaplan 2009). Local deforestation or landownership may have controlled the usage of mortar and building stones from different source areas.

Longer transport distances of > 10 km are seen for three localities: Ahaus-Wessum, Albersloh-Sendenhorst and Münster. The masonry of Ahaus-Wessum has been dated as late Santonian (Kaplan 2009). This correlates with the age obtained from the mortar, giving the source rocks a distance of 20 km (Fig. 8). For the church in Albersloh-Sendenhorst, glauconitic marl-limestones of the Baumberge Formation were transported over 30 km. Building stones of the masonry are from a different source (Ahlen Formation; Kaplan 2009). Again, the above listed factors (shortage of wood, landownership) may explain these different source areas. The chimney flank (Münster, sample 10) is of late Campanian age (Fig. 4), and the raw material can be attributed to the sandy marly limestones of the Baumberge Formation, being exposed at a distance of 10 km. Two possible source rocks of the Baumberge Formation were studied, which show significant differences in the relative abundances of *Watznaueria* (s4), *Prediscosphaera* (s4, s6) and *Micula* (s6; Fig. 7) and are thus very likely not exactly the same source rock of the chimney flank. Studies on samples of the Baumberge Formation documented drastic changes in the nannofossil content in the layers (from no nannofossils to 23 species; Fesl et al. 2005). A major problem lies in the primary variation of calcareous nannofossils throughout the sequence exposed in a given quarry. This sequence was often deposited over a time span of > 100,000 years. Relative abundances and diversity patterns can change from bed to bed on a scale of a few centimetres, reflecting primarily ecologic changes (e.g. summer, winter, warm/cold phases etc.) and also diagenetic variability. Individual samples taken from one bed in an outcrop are thus related to specific conditions, characterised by typical assemblages. It is therefore likely that not the right layer was studied here as a source rock.

In the current study, a limited number of samples was analysed for each of the historic building discussed. The raw material sources and technology may have changed throughout the architectural history of the buildings. Further studies and samples are needed to get a better understanding of the mortar production of each building.

Archaeothermometry

The absence of calcareous nannofossils in mortars from four historic sites (Bielefeld-Kirchdornberg, Warendorf-Einen, Rheda-Wiedenbrück, Meschede) can be explained in two different ways (Figs. 4 and 5). First, the source rocks used for producing the binder are barren of calcareous nannofossils in the first place. This applies for areas where carbonates older than Late Triassic are exposed, since nannofossils evolved first in the Late Triassic. The absence of nannofossils in Bielefeld-Kirchdornberg and in Meschede can be explained in this way. Near Bielefeld, carbonates of Triassic age crop out, which have been used as building stones in the masonry (Kaplan 2009). In Meschede, geologically, old limestones of Devonian age crop out (Thome 1968), which are barren of nannofossils. High burning temperatures may be seen as another cause for the absence of calcareous nannofossils, which only survive up to 900 °C (Falkenberg and Mutterlose 2022). For Warendorf-Einen and Rheda-Wiedenbrück, where Late Cretaceous limestones are exposed next to the churches, the absence of nannofossils is explained by calcination temperatures of 900 °C or higher.

In 24 out of 33 binders of mortar and mortar-based samples, preservation of calcareous nannofossils is poor with low abundances and diversities; only heat-resistant species like *W. barnesiae* or *E. floralis* are present. This argues for calcination temperatures of 900 °C or higher (Falkenberg and Mutterlose 2022; Table 4). The moderate preservation and the relatively high number of nannofossil species in the binder of mortar samples 16 and 17 (Warendorf-Freckenhorst) suggest burning temperatures < 900 °C. Sample 17 yields *Biscutum constans*, a small heterococcolith, which is destroyed at temperatures around 600 °C, thus indicating highest calcination temperatures of 500 to 600 °C (Falkenberg and Mutterlose 2022). Moderate preservation and diversity of calcareous nannofossils in the binder of mortar sample 25 (Soest; Figs. 5, 6 and 7) and the presence of the small heterococcolith *Zeugrhabdotus noeliae* and *Helicolithus* (Online Resource 4), which both disintegrate at temperatures between 500 and 750 °C, argue for burning temperatures of 500–700 °C. The absence of *Biscutum* indicates temperatures of 600–850 °C (Falkenberg and Mutterlose 2022) for this sample. The binder of mortar sample 29 (Paderborn) shows lower values for both diversity and the Shannon Index than the aggregate/lime lump from the same sample and the corresponding source rock (Fig. 7). These findings argue, in combination with the moderate-poor preservation (Fig. 6), the high relative abundances of *Watznaueria* and *Eprolithus* and the absence of *Biscutum*, for burning temperatures of 750–850 °C (Falkenberg and Mutterlose 2022; Table 4). Only rocks with good or good-moderate preserved calcareous nannofossils were used for the burning experiments; thus, no temperature ranges can

Table 4 Burning temperatures of the nine mortar and mortar-based samples. The estimates are based on calcareous nannofossil counting

Building	Sample ID	Lumps	Burning temperature	
			Binder	Lump/aggregate
Rheine, St. Dionysius	1	Ob, Ub/Agg	≥ 900 °C	≤ 500 °C
Legden-Asbeck, St. Margareta	5	Ob, Ub/Agg	≥ 900 °C	> 500–≤ 700 °C ?
Selm-Cappenberg, St. Johannes	20	Ob, Ub/Agg	≥ 900 °C	≤ 500 °C
Soest, St. Patrokli	25	Ob, Ub, Agg	> 600–≤ 750 °C	≤ 500 °C/ > 500–≤ 700 °C
Paderborn, Cathedral	26	Ob, Ub, Agg	≥ 900 °C	≤ 500 °C (close to 500 °C)
	27	Ob, Agg	≥ 900 °C	≤ 500 °C
Paderborn, Abdinghof Church	29	Ob, Ub, Agg	> 700–≤ 850 °C	≤ 500 °C
	30	Ob, Ub/Agg	≥ 900 °C	> 100–≤ 300 °C
Büren, St. Nikolaus	31	Ob, Ub/Agg	≥ 900 °C	> 100–≤ 300 °C

be given for source rocks with a primarily moderate or poor preservation. In the current study, all source rocks and lime lumps showed a good-moderate or good preservation. Ten samples (Figs. 4 and 5) did not provide any reliable temperature estimates, because either underburnt lime lumps or corresponding source rocks and thus the knowledge of the initial preservation are missing.

The presence of lime lumps in all but one sample provides clues to the burning temperature. Most common are lime lumps that closely resemble the binder but are missing aggregates (Fig. 6, marked with 1). These are either overburnt lumps or well-calcined lime, often showing cracks due to a slow carbonation process (Carran 2015). Co-occurring lumps with fossils and sedimentary structures (Fig. 6) are caused by low burning temperatures, indicating that the limestones thus experienced different temperature regimes during the quicklime production (Elsen 2006). Often, more than one type of lime lump can be found in one sample (Elsen 2006; Ingham 2011; Carran 2015). The co-occurrence of over- and underburnt lime lumps indicates an uneven heat distribution during the calcination process. A comparison of the calcareous nannofossils in the mortar and those coming from the corresponding source rock can supply more accurate information about the temperatures (Table 4).

Mortar samples 1, 20, 25, 26, 27 and 29 show equal high diversities, Shannon Indices, preservation and relative abundances for lime lumps/aggregates and corresponding source rocks (Figs. 4, 5, 6 and 7). These findings argue for burning temperatures of max. 500 °C, a value which is an important temperature threshold above which most nannofossils start to disintegrate (Falkenberg and Mutterlose 2022; Table 4). In mortar sample 25 (Soest), the high relative abundance of the heat-resistant nannolith *Eprolithus* in lump 3 (Fig. 7) and of the heat-resistant holococcolith *Lucianorhabdus* in lump 2 suggest burning temperatures of 500–700 °C (Table 4). This interpretation is supported by a low relative abundance of *Biscutum* in all three lumps/aggregates of sample 25 (Online Resource 4). Two of the three source rocks (samples s12, s13) provided higher relative abundances of the heat-resistant *Watznaueria* than their corresponding lime lumps/aggregates of mortar sample 25. This finding is contradicting to the implied higher burning temperatures and may argue for temperatures < 500 °C like the diversities and Shannon Indices. In mortar sample 26 (Paderborn), *Watznaueria* is slightly more common in the lime lump than in the corresponding source rock (sample s15), which argues for temperatures close to 500 °C (Falkenberg and Mutterlose 2022; Table 4). In mortar sample 27 (Paderborn), the values of *Eprolithus* are higher in the aggregates/lime lumps than in the corresponding source rocks (samples s14, 15), suggesting high burning temperatures. Relative low values of *Watznaueria* in the aggregates/lime lumps in comparison to the corresponding source rocks are, however, contradicting this view and argue again like the diversities and Shannon Indices for temperatures < 500 °C. Some minor differences of a few % in the relative abundances of all species in comparison to the initial relative abundances are also observed at temperatures lower than 500 °C (Falkenberg and Mutterlose 2022). This could explain the above-described differences here (Fig. 7). A second explanation asks for source rock quarries different to those sampled for the current study. The medieval quarries are nowadays no longer accessible; thus, outcrop samples have been collected from localities 10 km off.

In render sample 30 (Paderborn) and mortar sample 31 (Büren) diversities, Shannon Indices and relative abundances are close to those obtained from their corresponding source rocks with one exception. *Biscutum* has higher relative abundances (Fig. 7) in the lime lumps/aggregates than in the corresponding source rocks, indicating burning temperatures between 100 and 300 °C (Falkenberg and Mutterlose 2022; Table 4). In sample 31 (Büren), the relative abundance of *Watznaueria* is higher in the source rocks than in the corresponding lime lumps/aggregates. Again, samples

were not collected from the medieval historic quarries in Büren, which are no longer available, but from 10-km-distant quarries.

Mortar sample 5 (Legden-Asbeck) was compared to two potential source rock samples (Figs. 4 and 7). A much lower diversity and Shannon Index are seen in the aggregate/lime lump than in the two source rocks (Fig. 7); the preservation is the same (Fig. 4). The high relative abundances of the genus *Lucianorhabdus* in the lime lump/aggregate and the absence of *Biscutum* indicate burning temperatures of 500–700 °C (Falkenberg and Mutterlose 2022; Table 4). Nannoliths like *Micula* are also more heat resistant and here, *Micula* shows higher relative abundances in the source rocks than in the lime lump/aggregate (Fig. 7).

The approach to compare outcrop and corresponding mortar samples has specific limitations. A major problem lies in the primary variation of calcareous nannofossils throughout the sequence exposed in a given quarry. The composition of the exact same individual layers used for supplying the mortar is needed to provide more accurate burning temperatures. It is quite likely that different layers were mixed and used for the quicklime production, which further complicates the interpretation. Another problem is the yet unknown exact influence of the burning duration and atmosphere during the burning. The temperature given here are thus first estimates, more accurate data require burning experiments under controlled conditions.

Calcareous nannofossils in ultra-thin sections of mortars and mortar-based materials

For 19 out of 25 mortar and mortar-based samples, the ultra-thin sections provided more precise stratigraphic results than the corresponding smear slides. Similar ages have been obtained from five sample sets; in one case, the smear slide analysis provided a more precise age (sample 9; Online Resource 4). In another case (sample 29, Paderborn), the ultra-thin section and smear slide provided slightly different biostratigraphic ages. A UC9c age was obtained for the ultra-thin section and a slightly older UC9b age for the smear slide (Fig. 5; Online Resource 4).

As binder, lime lumps and aggregates can be studied in ultra-thin sections individually, this technique allows a much more differentiated provenance analysis of the three components. This approach further allows a direct comparison of nannofossil abundances and diversities of mortar components and the source rocks, thereby indicating a temperature range of the burning process of historic quicklime production.

The production of the < 10-µm ultra-thin sections is, however, very time consuming and expensive. Ultra-thin sections further require more material than simple smear slides, excluding this approach for critical materials where only minute amounts of < 1 g can be taken.

A comparison of calcareous nannofossils counted in an ultra-thin section and a smear slide of the chimney flank documents differences in the relative abundances encountered. The genus *Prediscosphaera* has much higher relative abundances in the ultra-thin section than in the smear slide, while the small genus *Biscutum* was not counted in the ultra-thin section but in the smear slide (Fig. 7). Smaller nannofossils are harder to spot in an ultra-thin section, while other bigger nannofossils are easier to recognise. This issue should be studied more in future.

Conclusion

The study of mortars and mortar-based materials of churches and historic buildings across the Münsterland allows the following conclusions:

1. Our data prove that for the construction of ten historic sites, locally occurring limestones have been mined for mortar production. The source rocks crop out in the vicinity of the buildings and were transported over a distance of 1–5 km. Four sites obtained their source rocks from a distance of more than 10 km. Factors explaining these rather long transport distances include the availability of wood or socioeconomic causes such as ownership of land and quarries.
2. Ultra-thin sections allow a much more precise age assignment and thereby a more accurate provenance analysis of the mortars than standard smear slides. In three ultra-thin sections, the study of the lime lumps/aggregates indicated that more than one source rock was used. A potential explanation for this feature is a mixture of leftover rocks or the combined burning of newly mined limestones and of old building stones.
3. The analysis of binder, lime lumps and aggregates encountered in a given mortar sample documents the presence of calcareous nannofossils in all three materials. The comparison of relative abundance, preservation and diversity data of nannofossils in these three components with data from source rocks supplied temperature ranges of the historic quicklime production for nine samples. Counting of calcareous nannofossils in the binder was possible in two samples, suggesting a max burning temperature of 600 to 750 °C in one case.
4. The ultra-thin section technique is a significant improvement in comparison to the standard smear slide method. Limitations are, however, seen in the difficulty to recognise smaller nannofossils and in the time consuming and expensive production of the ultra-thin sections.

Appendix

Taxonomy

Biscutum Black in Black and Barnes 1959

B. constans (Górka 1957) Black in Black and Barnes 1959

Calculites Prins and Sissingh in Sissingh 1977

Cretarhabdaceae Thierstein 1973

Eiffellithus Reinhardt 1965

Eprolithus Stover 1966

E. floralis (Stradner 1962) Stover 1966

Helicolithus Noël 1970

Kamptneriaceae Bown and Hampton 1997 in Bown and Young 1997

Lucianorhabdus Deflandre 1959

L. maleformis Reinhardt 1966

Micula Vekshina 1959

Prediscosphaera Vekshina 1959

Tranolithus orionatus (Reinhardt 1966a) Reinhardt 1966b

Watznaueria Reinhardt 1964

W. barnesiae (Black in Black and Barnes 1959) Perch-Nielsen 1968

Zeugrhabdotus Reinhardt 1965

Z. noeliae Rood et al. 1971

Supplementary information The online version contains supplementary material available at https://doi.org/10.1007/s12520-023-01840-2.

Acknowledgements The authors thank all the people who made the samplings in the churches possible. Special thanks go to Domprobst Monsignore J. Göbel (Paderborn) and Fürst M. zu Bentheim-Tecklenburg (Rheda). M. Huyer (LWL Münster) kindly provided material of historic buildings from Rheine, Münster, Albersloh-Sendenhorst and Selm-Cappenberg. We also thank G. Drozdzewski (Krefeld) for sending us the material from the historic building in Mönchengladbach. Special thanks go to Dr. Ulf Zinkernagel (Consulting Laboratory, Bochum), who kindly prepared the ultra-thin sections. We are grateful to L. Wulff, K. Stevens, R. Hoffmann (Ruhr-Universität Bochum) and R. Volkmann (GFZ, Potsdam) for the valuable discussions. Two reviewers improved an earlier version of this paper by thoughtful comments.

Author contributions Conceptualisation: Janina Falkenberg, Joerg Mutterlose; methodology: Janina Falkenberg, Ulrich Kaplan, Joerg Mutterlose; formal analysis and Investigation: Janina Falkenberg; visualisation: Janina Falkenberg; writing — original draft preparation: Janina Falkenberg; writing — review and editing: Joerg Mutterlose, Ulrich Kaplan; resources: Ulrich Kaplan, Joerg Mutterlose.

Funding Open Access funding enabled and organized by Projekt DEAL.

Data availability All relevant data are made available in the supplementary data files of this article.

Code availability Not applicable.

Declarations

Competing interests The authors declare no competing interests.

References

Bown PR, Young JR (1998) Introduction. In: Bown PR (ed) Calcareous Nannofossil Biostratigraphy. Kluwer, Dordrecht, pp 1–15

Boynton RS (1980) Chemistry and technology of lime and limestone, 2nd edn. John Wiley & Sons, New York

Burnett JA (1998) Upper Cretaceous. In: Bown PR (ed) Calcareous Nannofossil Biostratigraphy. Kluwer, Dordrecht, pp 132–199

Carran D, Hughes JJ, Leslie A, Kennedy C (2012) A short history of the use of lime as a building material - beyond Europe and North America. Int J Archit Herit 6(2):117–146

Carran D (2015) The characterisation of historic mortars with a focus on provenance. Dissertation, University of the West of Scotland, Paisley

Dix B (1982) The manufacture of lime and its uses in the western Roman provinces. Oxford J Archaeol 1(3):331–345

Dölling B, Dölling M, Hiss M, Berensmeier M, Püttmann T (2018) Upper Cretaceous shallow-marine deposits of the southwestern Münsterland (Northwest Germany) influenced by synsedimentary tectonics. Cretac Res 87:261–276

Drozdzewski G (1995) Geologischer Bau. In: Drozdzweski G, Hiss M, Lehmann F, Michel G, Skupin K, Staude H, Thiermann A, Dahm-Arens H, Finke W (eds) Geologie im Münsterland. Geologisches Landesamt Nordrhein-Westfalen, Krefeld, pp 14–18

Elsen J (2006) Microscopy of historic mortars – a review. Cem Concr Res 36:1416–1424

Elsen J, Mertens G, Van Balen K (2011) Raw materials used in ancient mortars from the Cathedral of Notre-Dame in Tournai (Belgium). Eur J Mineral 23:871–882

Falkenberg J, Mutterlose J (2022) Towards a better understanding of historic mortar production – burning experiments on calcareous nannofossils. Archaeol Anthropol Sci 14(4):66. https://doi.org/10.1007/s12520-022-01535-0

Falkenberg J, Mutterlose J, Kaplan U (2021) Calcareous nannofossils in medieval mortar and mortar-based materials: a powerful tool for provenance analysis. Archaeom 63(1):19–39

Fesl S, Bornemann A, Mutterlose J (2005) Die Baumberge-Schichten (Ober-Campan) im nordwestlichen Münsterland – Biostratigraphie und Ablagerungsraum. Geol Paläont Westf 65:95–116

Gardin S, Krystyn L, Richoz S, Bartolini A, Galbrun B (2012) Where and when the earliest coccolithophores? Lethaia 45:507–523

Geisen M, Bollmann J, Herrle JO, Mutterlose J, Young JR (1999) Calibration of the random settling technique for calculation of absolute abundances of calcareous nannoplankton. Micropaleontol 45(4):437–442

Goren Y, Goldberg P (1991) Petrographic thin sections and the development of Neolithic plaster production in northern Israel. J Field Archaeol 18(1):131–140

Goren Y, Goring-Morris AN (2008) Early pyrotechnology in the Near East: experimental lime-plaster production at the pre-pottery Neolithic B site of Kfar HaHoresh. Israel Geoarchaeol 23(6):779–798

Grupe O (1933) with contributions by Koert W, Stach E, Ihnen K, Erläuterungen zur Geologischen Karte von Preußen und benachbarter deutscher Länder. Blatt Minden, Preußische Geologische Landesanstalt, Berlin

Hiss M (1995) Kreide. In: Drozdzweski G, Hiss M, Lehmann F, Michel G, Skupin K, Staude H, Thiermann A, Dahm-Arens H, Finke W (eds) Geologie im Münsterland. Geologisches Landesamt Nordrhein-Westfalen, Krefeld, pp 41–65

Hiss M, Mutterlose J (2010) Field trip E6: Cretaceous geosites of the eastern Ruhr area and the southern Münsterland. In: Mügge-Bartolović V, Röhling H-G, Wrede V (eds) Geotop 2010 – Geosites for the public. Paleontology and conservation of geosites. Schriftenreihe der Deutschen Gesellschaft für Geowissenschaften, Vol 66, Hannover, pp 168–183

Hooper WD, Ash HB (1939) Marcus Porcius Cato Marcus Terentius Varro. William Heinemann Ltd, Harvard University Press, London, De Re Rustica

Hughes JJ, Swift DS, Bartos PJM, Banfill PFG (2002) A traditional vertical batch lime kiln: thermal profile and quicklime characteristics. In: Throop D, Klinger RE (eds) Masonry: Opportunities for the 21st Century, ASTM STP 1432. American Society for Testing and Materials, West Conshoshocken, pp 73–87

Ingham JP (2011) Geomaterials under the microscope: a colour guide. Manson Publishing, London

Jordan RW (2009) Coccolithophores. In: Schaechter M (ed) Encyclopedia of Microbiology. Elsevier Academic Press, Oxford, pp 593–605

Kaplan U (2009) Naturbausteine historischer Bauwerke des Münsterlandes und seiner angrenzenden Gebiete. Geol Paläont Westf 73:7–178

Klostermann J, Paas W, Prüfert J, Schlimm W, Thiermann A, Zeller M (1990) Erläuterungen zu Blatt C 5102 Mönchengladbach – Geologische Karte von Nordrhein-Westfalen 1:100000. Geologisches Landesamt Nordrhein-Westfalen, Krefeld

Kommende Steinfurt (1686–1722) Angelegenheiten der Eingesessenen des Ksp. Rheine, insb. Emsbrücke, Hölting und Kalkbrennen, betr. Laufzeit 1686–1722. Bur.H.Ak. 505. Vereinigte Westfälische Adelsarchive e.V., Landesarchiv NRW Abteilung Westfalen, Münster

Kühn H (1986) Naturwissenschatfliche Untersuchungen von Mörtelproben. In: Lobbedey U (ed) Die Ausgrabungen im Dom zu Paderborn 1978/80 und 1983. Landschaftsverband Westfalen-Lippe, Münster, pp 309–317

Kumar GS, Ramakrishnan A, Hung Y-T (2007) Lime calcination. In: Wang LK, Hung Y-T, Shammas NK (eds) Handbook of Environmental Engineering, vol 5. Advanced Physicochemical Treatment Technologies. Humana Press Inc., Totowa, New Jersey, pp 611–633

Lobbedey U (1986) Die Ausgrabungen im Dom zu Paderborn 1978/80 und 1983. Landschaftsverband Westfalen-Lippe, Münster

Lübke N, Mutterlose J, Börste N, Kaplan U (2018) A micropalaeontologically based provenance analysis of masonry and floor tiles from the medieval cathedral of Paderborn (Northern Germany). Archaeom 60(6):1170–1183

Miller J (1988) Microscopical techniques: I. Slides, slices, stains and peels. In: Tucker M (ed) Techniques in Sedimentology. Blackwell Science Publications, Oxford, London, Edinburgh, Boston, Melbourne, pp 86–107

Morgan MH (1914) Vitruvius: the ten books on architecture. Harvard University Press, Cambridge

Müller G (1964) Sediment-Petrologie 1. Methoden der Sedimentuntersuchung. Schweizerbart'sche Verlagsbuchhandlung, Stuttgart, Teil

Pavía S, Caro S (2008) An investigation of Roman mortar technology through the petrographic analysis of archaeological material. Constr Build Mater 22:1807–1811

Perch-Nielsen K (1985) Mesozoic Calcareous Nannofossils. In: Bolli HM, Saunders JB, Perch-Nielsen K (eds) Plankton Stratigraphy, vol 1. Cambridge University Press, Cambridge, pp 329–426

Quinn PS (2008) The occurrence and research potential of microfossils in inorganic archaeological materials. Geoarchaeol 23(2):275–291

Quinn PS, Day PM (2007) Calcareous microfossils in Bronze Age Aegean ceramics: illuminating technology and provenance. Archaeom 49(4):775–793

Roth PH, Thierstein H (1972) Calcareous nannoplankton: leg 14 of the Deep Sea Drilling Project. In: Hayes DE, Pimm AC et al (eds) Initial Reports of the Deep Sea Drilling Project, vol 14. US Government Printing Office, Washington, pp 421–485

Roth PH (1983) Jurassic and Lower Cretaceous calcareous nannofossils in the western North Atlantic (Site 543): biostratigraphy, preservation and some observations on biogeography and paleoceanography. In: Sheridan RE, Gradstein FM et al (eds) Initial Reports of the Deep Sea Drilling Project, vol 76. US Government Printing Office, Washington, pp 587–621

Shannon CE, Weaver W (1949) The mathematical theory of communication. University of Illinois Press, Urbana

Skupin K (1995) Tertiär. In: Drozdzweski G, Hiss M, Lehmann F, Michel G, Skupin K, Staude H, Thiermann A, Dahm-Arens H, Finke W (eds) Geologie im Münsterland. Geologisches Landesamt Nordrhein-Westfalen, Krefeld, pp 66–70

Skupin K, Staude H (1995) Quartär. In: Drozdzweski G, Hiss M, Lehmann F, Michel G, Skupin K, Staude H, Thiermann A, Dahm-Arens H, Finke W (eds) Geologie im Münsterland. Geologisches Landesamt Nordrhein-Westfalen, Krefeld, pp 71–95

Skupin K, Speetzen E, Zandstra JG (1993) Die Eiszeit in Nordwestdeutschland. Zur Vereisungsgeschichte der Westfälischen Bucht und angrenzender Gebiete, Geologisches Landesamt Nordrhein-Westfalen, Krefeld

Stark J, Wicht B (1998) Geschichte der Baustoffe. Bauverlag GmbH, Wiesbaden, Berlin

Thome KN (1968) with contributions by Mertens H, Rehagen H-W, Wolf M, Erläuterungen zu Blatt 4615 Meschede – Geologische Karte von Nordrhein-Westfalen 1:25000. Geologisches Landesamt Nordrhein-Westfalen, Krefeld

Torraca G (1995) Lime technology in architectural conservation. Lime News (journal of the Building Limes Forum) 4(1):34–41

Tucker M (1985) Einführung in die Sedimentpetrologie. Enke Verlag, Stuttgart

Voigt S, Wagreich M, Surlyk F, Walaszczyk I, Uličný D, Čech S, Voigt T, Wiese F, Wilmsen M, Niebuhr B, Reich M, Funk H, Michalík J, Jagt JWM, Felder PJ, Schulp AS (2008) Cretaceous. In: McCann T (ed) The Geology of Central Europe, vol 2. Mesozoic and Cenozoic. The Geological Society, London, pp 921–997

von Salis K (1995) Calcareous nannofossils in the arts. J Nannoplankton Res 17(2):88–90

Webb TL, Krüger JE (1970) Carbonates. In: Mackenzie RC (ed) Differential thermal analysis. Academic Press, London, New York, pp 303–341

Wegner T (1927) Geologie der Münsterschen Ebene. In: Wegner T (ed) Westfalenland. Eine Landes- und Volkskunde Westfalens, Vol IV. Beiträge zur Westfälischen Heimatkunde, Münster, pp 1–44

Young JR (2020) Coccoliths and other marine microfossils in microparticle analysis. In: Henry AG (ed) Handbook for the Analysis of Micro-Particles in Archaeological Samples. Springer, Cham, pp 7–21

Young JR, Henriksen K (2003) Biomineralization within vesicles: the calcite of Coccoliths. Rev Mineral Geochem 54(1):189–215